Journal of Critical Reviews

ISSN- 2394-5125 Vol 7, Issue 4, 2020

Review Article

CHECKERBOARD ELECTROMAGNETIC BAND GAP (EBG) STRUCTURED S-SHAPED ANTENNA FOR WEARABLE APPLICATIONS

[1]Kunapareddy Koteswara Rao, [2]Pasumarthy Nageswara Rao, [3]Vangala Sumalatha

[1]Research Scholar, Department of ECE, JNTU Anantapur, AP, India
[2]Professor, Department of ECE, Vardhaman College of Engineering Hyderabad
[3]Professor, Department of ECE, JNTU Anantapur, AP, India

Received: 13.12.2019 ***Revised: 15.01.2020*** ***Accepted: 18.02.2020***

Abstract

A miniaturized wearable antenna with a compact EBG with checkerboard structure is designed. The structure is placed on a denim jeans material with thickness of 0.7mmand having dielectric constant of 1.7 and a loss tangent of 0.02. The antenna operates at a frequency of 2.5 GHz and has 0.33GHz bandwidth and 13.2% impedance bandwidth for ISM band applications. The prototype is robust as well as compact and adheres to the wearable applications. The EBG is used to improve the gain and reduces the Specific Absorption Rate (SAR) which is an essential in wearable applications. The gain of 6.5dBi and SAR of 0.0312W/Kg is achieved, satisfying the required conditions of the antenna in the presence and absence of EBG to assess the changes caused in the performance of the antenna due to the insertion of EBG.

Keywords: Body Area Networks, Human Phantom Model, Specific Absorption Rate, Wearable Antenna

DOI: http://dx.doi.org/10.31838/jcr.07.04.115

INTRODUCTION

All modern wireless communication systems need to utilize a low-profile radiator. It is due to the reduction in size of the devices and they should have small radiating structure. This is where the microstrip patch antennas comes into picture. Microstrip patch antenna has low profile which can be fabricated with ease and can be easily integrated with microwave circuits. The main disadvantage of the microstrip patch antenna is that it has very low gain. So much research has been performed to improve the gain of the antenna [1]. Some of the techniques used to improve the performance of the antenna are to include slots in the patch, introducing a parasitic patch, Stacked Dielectric layers and EBG structures. Electromagnetic bandgap (EBG) materials are one of the most rapidly advancing materials. They can change the propagation of electromagnetic waves to a level which was not possible earlier [2]. EBG structures are defined as artificial periodic structures that avert or assist the propagation of electromagnetic waves in a specified band of frequencies for all incident angles and all polarization states [3]. EBG structures are also known as high impedance surface due to their ability to suppress the surface wave at certain operational frequencies. Electromagnetic Band Gap (EBG) structures produce a lot of design alternatives for researchers working in the area of microwave and photonics [4-5].

Generally, EBG structures may be a bit complex but here we design an EBG structure with the concept of wearable antenna. The area of wearable computing systems is rapidly emerging due to its extensive applications in several areas. It is used in health monitoring for elderly/ children, observing human vital signs, physical training, tracking and emergency rescue systems, military, telemedicine, sports, and tracking [6]. An antenna plays a very important role in a wearable device. Since the antenna is within a very close proximity to the human body, the performance of the antenna must be taken into consideration like the structural bending, mismatch and losses caused by the body, while at the same time, sustains the performance. Also, it must be low-profile, robust and light weight. The radiation from the wearable antenna should present the least specific absorption rate (SAR) [7] above human layers and satisfy the safety requirements. A planar monopole with a 2 x 1 array of Electromagnetic Band Gap (EBG) structures is used. The reflection phase of a single EBG unit cell is presented [8]. A design of miniaturized multi-band 1 x 2 patch antenna array with electromagnetic band gap (EBG) for wideband operation has been studied.[9] The proposed antenna consists of three unequal arms fed by CPW-to-slot line transitions for ISM band applications. A novel electronically tunable two-layer slot-patch one-dimensional Electromagnetic Bandgap (EBG) structure with significantly simplified biasing network has been studied [10]. A wearable circular ring slot antenna with electromagnetic bandgap (EBG) structure for wireless body area network (WBAN) application is proposed. [11]. The design of a dual-band wearable fractal-based monopole patch antenna integrated with an electromagnetic bandgap (EBG) structure is presented. [12]. A dual band antenna with EBG structure in application to wearable communication system is investigated. A dual band EBG with two rectangular rings is designed [13]. A coplanar waveguide miniaturized wearable antenna is implemented in textile materials. To increase the performance of the antenna and to control the specific absorption rate, an artificial magnetic conductor (AMC) is implemented as a reflector plane [14]. A novel design of a uniplanar compact electromagnetic bandgap (EBG) for millimeter-wave wearable antennas is presented. The unit cell of the EBG has a flexible fractal design, which is easily fabricated at millimeter-scale [15-17]. The technology to design and develop the printed antennas has been continuously altered from the structural view of configuration to antenna features improvement. EBG structures have play a very important role to improve the features of printed antennas [18-21]. "I"-typed EBG units with varying size and center distance are used. It is a

method proposed to implement miniaturization by reducing the second half of the tapered EBG without giving up on bandwidth [22-23].

A low-profile antenna integrated with a checkerboard EBG for medical application is presented in this letter. The main objective is to reduce the size of the antenna, but the output should be intact. The dimensions of the antenna are 20 x 30 x 0.7 mm^3. The checkerboard EBG which is a combination of both squares and circles which is very much easy to implement. The design of the antenna and EBG structure are presented in Section 2. Analysis of the antenna on EBG plane is discussed in Section 3.

Antenna and EBG Design

The microstrip patch antenna proposed in this letter is acquired with the help of the iterations shown in the Fig 1. In the first iteration we consider a rectangular patch with the area of 16 x 20 mm with a denim substrate of thickness 0.7 mm and dielectric constant of 1.7. which doesn't show any reflection coefficient. So, aiming for better performance a slot is introduced in the second topology. This topology obtains a better performance compared to the other first iterations as it obtains an output at 2.5 GHz. Aiming better bandwidth slots are introduced in both upper part radiating patch and the corners edges are truncated

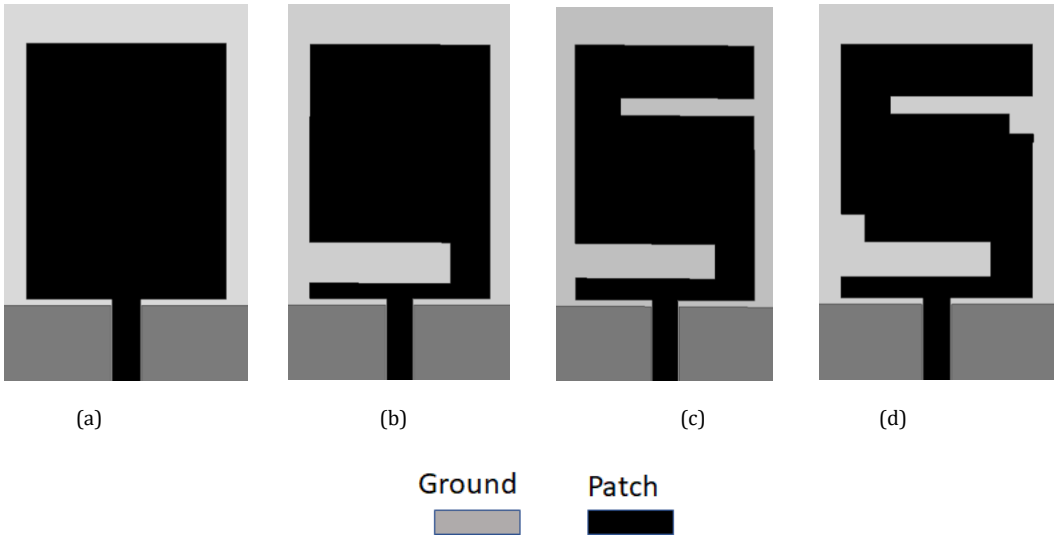

Fig1. (a) Iteration 1 (b) Iteration 2 (c) Iteration 3 (d) Proposed Antenna

Antenna Design

The S-shaped microstrip monopole antenna fed by a coplanar waveguide is designed by using HFSS tool. The antenna resonates at the ISM band frequency applications of 2.5 GHz. The antenna is mounted on a 0.7 mm thick denim material as a substrate with a dielectric constant of 1.7 and loss tangent of 0.02 as illustrated in Fig 2. The overall dimensions of the antenna are 20 x 30 x 0.7 mm^3. As we can see this antenna is compact and easy to design compared to other existing prototypes. The parameters of the antenna are given in Table 1. The width and length of the antenna are calculated with the help of the following equations [28]

$$W = \frac{1}{2 f_r \sqrt{\mu_0 \varepsilon_0}} \sqrt{\frac{2}{\varepsilon_r + 1}} = \frac{\upsilon_0}{2 f_r} \sqrt{\frac{2}{\varepsilon_r + 1}} \quad (1)$$

Where f_r is operating frequency and υ_0 is free space velocity of light

$$L = \frac{1}{2 f_r \sqrt{\varepsilon_{reff}} \sqrt{\varepsilon_0 \mu_0}} - 2\Delta L \quad (2)$$

where the equations of ε_{reff}, L_{eff} and ΔL are given below

EBG Design

Considering the compactness of the antenna EBG designed also need to be compact in design. So, the two EBG structures square and a circle are put together and considered as a single EBG. The square metallic patch of EBG1 has dimensions of 7.0 mm x 7.0 mm, thus, the separation between the patches is 0.5 mm and the circular metallic patch of EBG2 has diameter of 6.0 mm, the separation between the patches is 1.5 mm is located on the top of a thick denim material as a substrate with a dielectric constant of 1.7 and loss tangent of 0.02 as illustrated in Fig 2.

$$\frac{\Delta L}{h} = 0.412 \frac{(\varepsilon_{reff} + 0.3)\left(\frac{W}{h} + 0.264\right)}{(\varepsilon_{reff} - 0.258)\left(\frac{W}{h} + 0.8\right)} \quad (3)$$

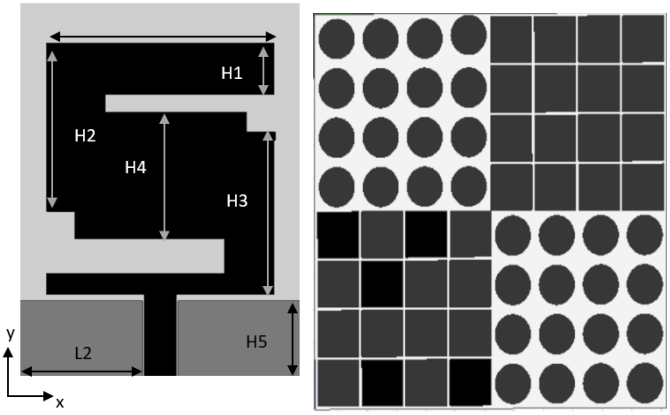

(a) **(b)**

Fig 2. (a) Proposed antenna (b) EBG for the proposed antenna

Table 1: Parameters of the antenna.

Parameters	H_1	H_2	H_3	H_4	H_5	L_1	L_2
Values(mm)	4.14	13.4	12.9	10.1	6.1	16	8.75

RESULTS AND DISCUSSIONS

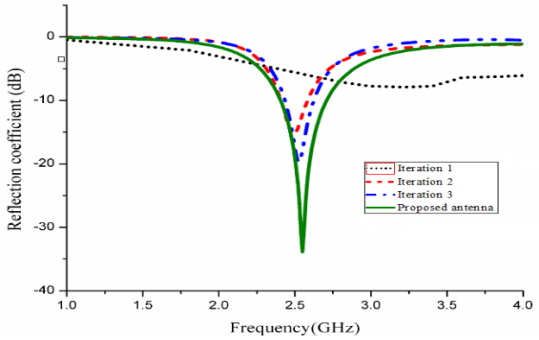

Fig 3. Reflection coefficient of iterations of the proposed antenna

The iteration results of the proposed antenna are presented in the Fig.3. The reflection coefficient of the first iteration of the antenna doesn't show any operating frequency so the antenna is modified by placing the rectangular slot in the radiating patch with which the reflection coefficient of the antenna is operated at the resonating frequency at 2.5 GHz with minimum S_{11} of -13dB with bandwidth of 0.17 GHz. Iteration 3 of the antenna shows the operating frequency ranging from 2.44-2.62 GHz with bandwidth of 0.24 GHz. The proposed antenna operates in the frequency range of 2.35-2.68 GHz with bandwidth of 0.33 GHz and resonates at the frequency of 2.5 GHz with minimum S_{11} OF -33dB.

Parametric analysis

The distance between the antenna and EBG is varied from 0mm to 35mm at 5mm intervals and the results are shown in the Fig 4. As the distance between the antenna and EBG increases the output obtained is better. When the distance from the EBG to antenna ranges from 0mm to 20mm the antenna does not radiate at all. At 25mm the antenna starts to radiate. And as the distance is increased to 30mm and 35mm the antenna starts exhibiting higher radiation. At 35mm the antenna exhibits highest radiation.

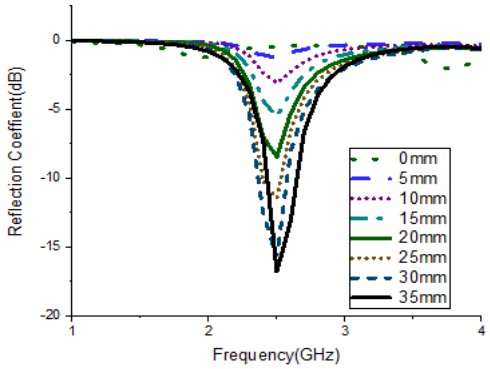

Fig 4. Parametric analysis for the distance between the antenna and EBG

To study the effect of the width of the patch on the antenna width l_5 is varied from 15mm to 18mm with an interval of 1mm. At 15mm the output is obtained at 2GHz, at 17mm output is obtained at 2.7GHz and at 18mm the output is obtained at 2.9GHz. The above three frequencies are not eligible for the applications which are aimed when the prototype is designed. So 16mm is considered as the width of the patch antenna. The results are shown in the Fig 5

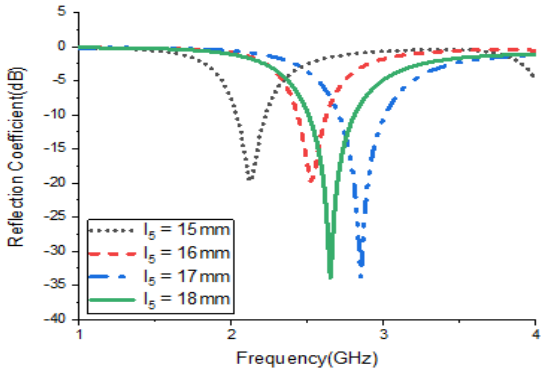

Fig 5. Parametric analysis of l_5

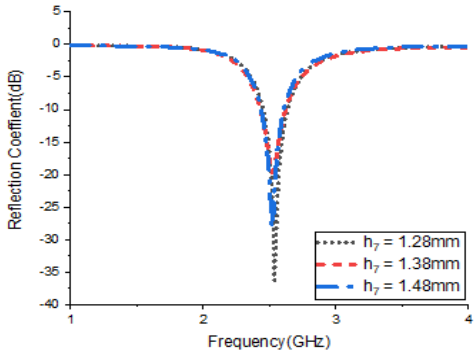

Fig 6. Parametric analysis of h_7

The length of the slot1 (h_7) is varied to assess the change in the antenna results obtained in the Fig 6. It is varied from 1.28mm to 1.48mm at an interval of 0.1mm. When h_7 is 1.38mm or 1.48 mm the results obtained are not as desired compared to the result obtained at 1.28mm.

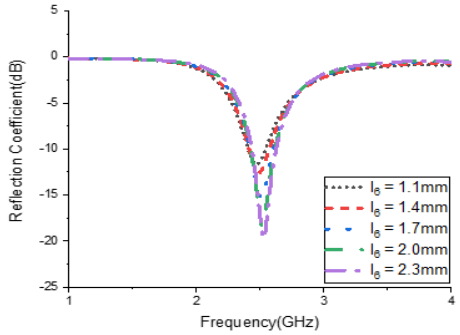

Fig 7. Parametric analysis of l_6

Variation of feed width always has some effect on the results obtained. In Fig 7 the results are shown from which the changes according to the changes in feed width are assessed. As the feed width increases the radiation of the antenna increases. The feed width l_6 is varied from 1.1mm to 2.3mm at an interval of 0.3mm.

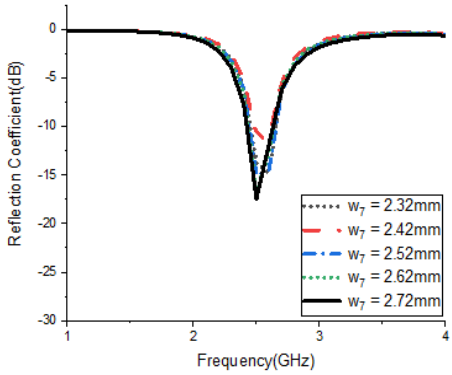

Fig 8. Parametric analysis of w_7

The length of the slot2 (w_7) is varied from 2.32mm to 2.72mm at an interval of 0.1mm to assess the changes in the results obtained which is shown in Fig 8. The output obtained when w_7 is considered as 2.72mm is better compared to the other values that are taken.

Compression of simulated and measured results

The experimental results of the proposed antenna are procured. The simulation and experimental results are acquired with the help of high frequency structure simulator (HFSS) and vector network analyzer. Fig 9 compares the performance of the proposed antenna for simulation and measurement. The measured antenna provides the operating frequency of 2-2.82 with operating bandwidth of 0.82 GHz without EBG and similarly with EBG structure antenna operates in the frequency range of 2.12-3.0 GHz with bandwidth of 0.88 GHz.

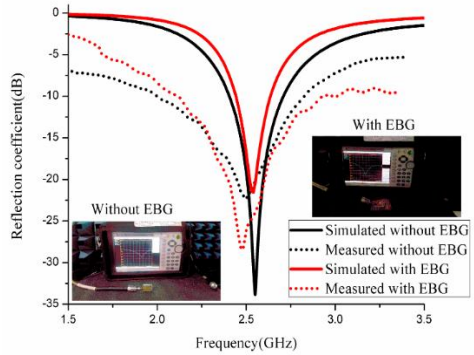

Fig 9. Reflection Coefficient of the antenna simulated and measured.

Gain and Efficiency of Proposed Antenna

In Fig 10 presents gain of the antenna with EBG and the gain of the antenna without EBG are compared. The gain (6.5dBi) of the antenna with EBG and the gain (1.8dBi) of the antenna without EBG are set against each other than the gain of the antenna with EBG is comparatively high. It is also same in the case of efficiency which is shown in Fig 11. The efficiency (97%) of the antenna

with EBG is more in contrast to the efficiency (86%) of the antenna without EBG.

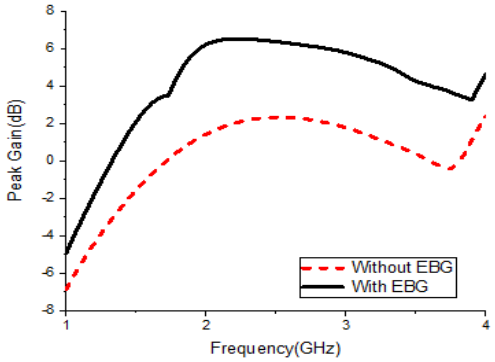

Fig 10. Gain of the antenna

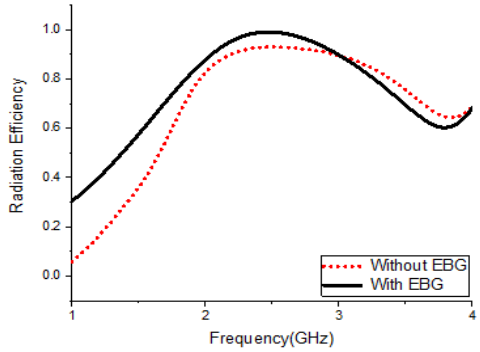

Fig 11. Radiation Efficiency of the antenna

Radiation Pattern of Proposed Antenna

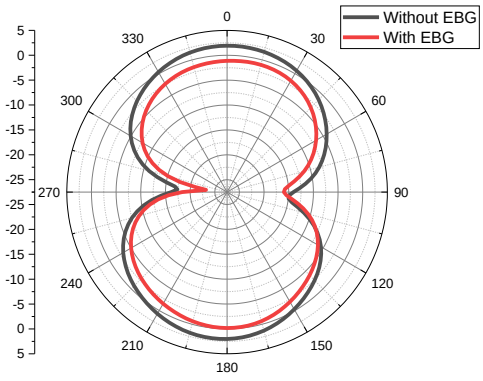

(a)

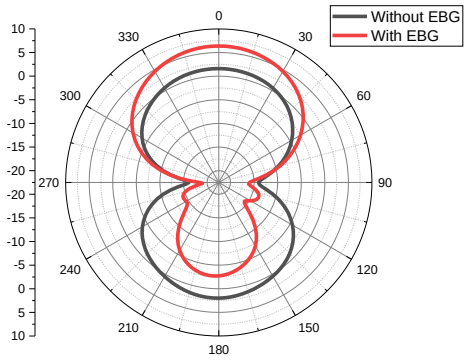

(b)

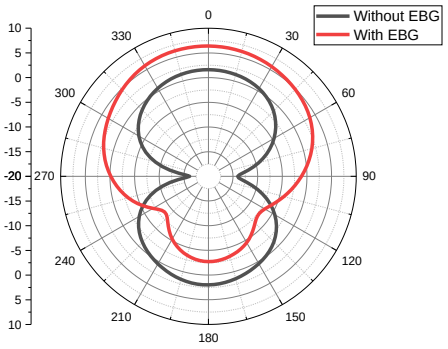

(c)

Fig 12. (a) Radiation pattern in XY direction (b) Radiation pattern in YZ direction (c) Radiation pattern in ZX direction

The radiation pattern in XY, YZ and ZX directions are shown in the Fig 12. The radiation pattern of antenna without EBG is compared with the radiation pattern of the model with EBG in XY, YZ, ZX directions. The radiation patterns for the antenna in the absence of EBG is a dipole in all the three directions considered, whereas in the presence of EBG the pattern in XY and YZ direction is dipole, while omnidirectional in ZX direction. Two patterns in all the directions are compared and it is observed that the radiation of the antenna is high in the presence of EBG.

Current Distribution

Fig 13 shows the current distribution of the antenna proposed at 2.45 GHz. The surface current is concentrated around the Coplanar Waveguide feed line and a part of the ground surface and the surface of the S-shaped antenna near the feed line and is distributed along less to left side of the feed and more to the right side and it follows the shape of the antenna. Current density reduces as it travels away from the feed line. The current distribution on the EBG is high for the elements in the edge and minimum for the elements in the center. It is also observed that the rectangular elements have comparatively high distribution than circular elements.

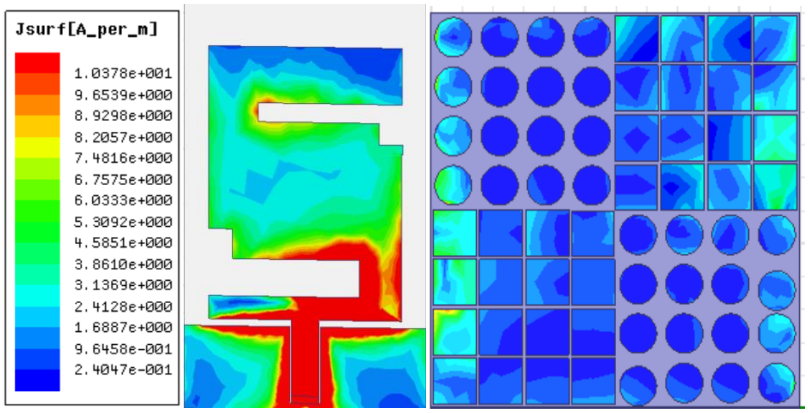

Fig 13. Current distribution of the model

ANALYSIS FOR WEARABLE APPLICATIONS

The Specific Absorption Rate of the proposed antenna is observed with and without EBG structure. A three layered cylindrical phantom structure is considered. Skin, fat and muscle are the three structures of the phantom layer and their dielectric constants are presented in the Table.2. The phantom analysis is used to estimate the amount of perturbation caused to the tissues in the human body due to the electromagnetic waves.

There are two standards at present which are required to be consider when the SAR is estimated. First one is IEEEC95.1-1999 standard. This restricts cylinder shape of 1-g tissue to have radiation less than 1.6 w/kg. According to the second standard, that is, IEEEC95.1 -2005 it restricts cylinder shape 10-g tissue to have radiation less than 2w/kg. The second standard, that is, IEEEC95.1 -2005 is considered to estimate SAR. CST Microwave studio simulation is used to analyze SAR of the antenna. The dielectric properties of skin fat and tissue are assigned to three layers of cylinders of phantom structure to assess the SAR on the human body. Since the antenna is not directly placed on the human body. It is placed at 20mm from the human body with an input power of 0.5W. The temperature within the human body increases with respect to the absorbed electric field over a period. So, SAR can be calculated using the formula mentioned [24-27]

$$SAR = \frac{C\Delta t}{\Delta T} \qquad (4)$$

where C is heat capacity of the tissue (J/kg/K), ΔT is temperature rise (K) and Δt is the short time exposure. The SAR values are

noted in the Fig.14 and Fig.15 shows the antenna placed on the three-layered model with and without the EBG structure. The SAR values observed without the EBG structure are 2.59 W/Kg and with EBG structure it is observed around 0.0312 W/Kg. The reduction of SAR values is observed with the placement of EBG structure in between the antenna and three-layered model.

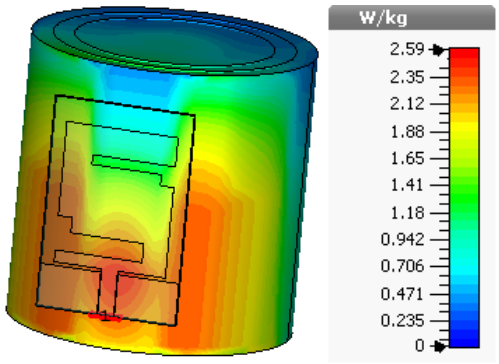

Fig 14. Specific Absorption Rate of the antenna without EBG

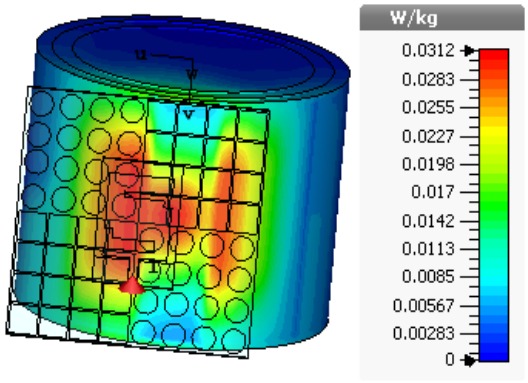

Fig 15. Specific Absorption Rate of the antenna with EBG

Table 2: Parameters of Human Phantom Model

Parameters	Skin	Fat	Muscle	Bone
Dielectric Constant	37.95	5.27	52.67	18.49
σ(S/m)	1.49	0.11	1.77	0.82
Density(kg/m3)	1001	900	1006	1008
Thickness(mm)	2	5	20	13

Bending Analysis

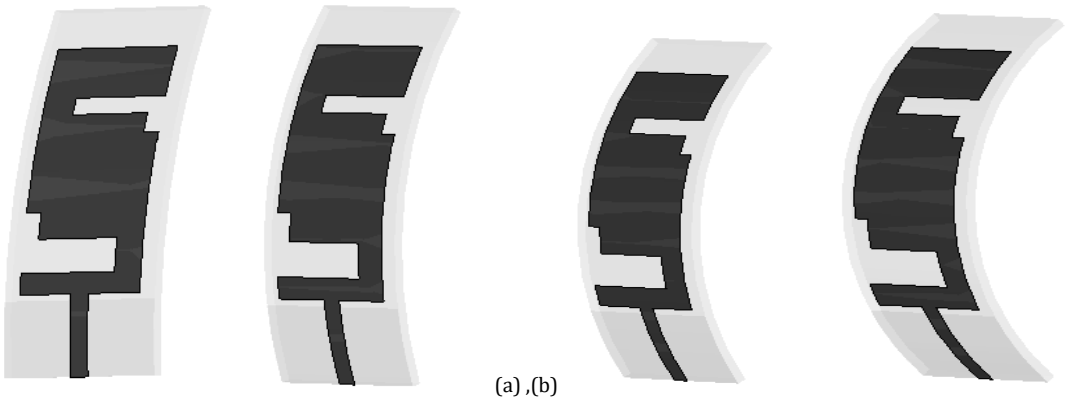

Fig 16. (a) Bending analysis at an angle10^0 (b) Bending analysis at 30^0 (c) Bending analysis at 45^0 (d) Bending analysis at 60^0

As the prototype is fabricated using a wearable material the bending of the antenna is most likely considered to estimate the efficiency of the antenna which is considered in this letter. So, the prototype is arced with different angles altering from 10 degrees to 60 degrees which is shown in the Fig 16 and the productiveness of the antenna is verified with the help of reflection coefficient shown in the Fig.17 where there is small variation in the reflection coefficient.

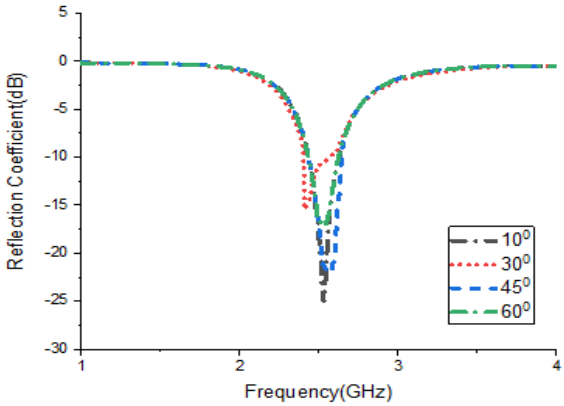

Fig 17. Reflection coefficient for Bending analysis

Table 3. Comparison of proposed antenna opposite other reference antennas

Reference	Resonating Frequency (GHz)	Material	Fractional Bandwidth (%)	Gain (dBi)	Reflect Plane	AMC area (mm* mm)
[18]	2.45	Rogers 5870	1.2	1.77	-	98 x 63
[20]	2.4	Latex	2	4.12	AMC	50 x 50
[21]	2.45	Taffeta fabric	5.1	4.2	-	33 x 26
[22]	2.45	Polyimide	18	4.8	AMC	45 x 30
[23]	2.4	PDMS	27	5.2	-	50 x 50
[24]	2.45	Jeans	5.08	-	EBG	150 x 150

[25]	2.45	Photo Fabric	4	0.86	EBG	127 x 87
[27]	2.45	Felt	15	2.5	AMC	100 x 100
This work	2.5	Jeans	13.2	6.5	EBG	60 x 60

Table.3 presents the comparison of the proposed work with the previous literature. The antenna designed on the jeans material and provides the impedance bandwidth of 13.2% and gain of 6.5 dBi which is high compared to the previous work. The EBG structure designed on the jeans material is compact in size and helps in reduction of SAR values.

CONCLUSIONS

A S-shaped antenna with a checkerboard EBG is designed and fabricated in this majuscule. The paradigm has a volume of 60 x 60x 0.7 mm^3 and is formulated with a denim substrate with a dielectric constant of 1.7. The peak gain obtained for the antenna when EBG is present is 6.5dBi and 1.3dBi in the absence of EBG. The SAR for the antenna without EBG is 2.59 W/kg and 0.312 W/kg in the presence of EBG structure for 10-g tissue with the help of a human phantom model. Among others the antenna is robust, light weighed and easy to fabricate compared to most of the other works which are shown in the table which make this prototype a worthy choice for different medical applications.

REFERENCES

1. Kuo, J. S., & Hsieh, G. B. (2003). Gain enhancement of a circularly polarized equilateral-triangular microstrip antenna with a slotted ground plane. *IEEE Transactions on Antennas and Propagation*, *51*(7), 1652-1656.
2. Yang, L., Fan, M., Chen, F., She, J., & Feng, Z. (2005). A novel compact electromagnetic-bandgap (EBG) structure and its applications for microwave circuits. *IEEE Transactions on Microwave Theory and Techniques*, *53*(1), 183-190.
3. Baccarelli, P., Burghignoli, P., Rezza, F., Galli, A., Lampariello, P., Paarulotto, S., & Valerio, G. (2007). Dispersive analysis of wide-bandstop compact EBG microstrip lines for filter applications. *Proceedings ISMOT 2007*.
4. Kshetrimayum, R. S., & Zhu, L. (2006, July). EBG design using FSS elements in rectangular waveguide. In *ACES* (Vol. 21, No. 2).
5. Verma, R., & Daya, K. S. (2011). Effect of forbidden bands of electromagnetic bandgap engineered ground plane on the response of half wavelength linear microwave resonator. *Journal of Applied Physics*, *109*(8), 084505.
6. Yang, H. L., Yao, W., Yi, Y., Huang, X., Wu, S., & Xiao, B. (2016). A dual-band low-profile metasurface-enabled wearable antenna for WLAN devices. *Progress In Electromagnetics Research*, *61*, 115-125.
7. Abd-Alhameed, R. A., Excell, P. S., & Mangoud, M. A. (2005). Computation of specific absorption rate in the human body due to base-station antennas using a hybrid formulation. *IEEE Transactions on Electromagnetic Compatibility*, *47*(2), 374-381.
8. Abbasi, M. A. B., Nikolaou, S. S., Antoniades, M. A., Stevanović, M. N., & Vryonides, P. (2017). Compact EBG-backed planar monopole for BAN wearable applications. *IEEE Transactions on Antennas and Propagation*, *65*(2), 453-463.
9. Malekpoor, H., & Jam, S. (2018). Design, analysis, and modeling of miniaturized multi-band patch arrays using mushroom-type electromagnetic band gap structures. *International Journal of RF and Microwave Computer-Aided Engineering*, e21404.
10. Mavridou, M., Feresidis, A. P., & Gardner, P. (2016). Tunable double-layer EBG structures and application to antenna isolation. *IEEE Transactions on Antennas and Propagation*, *64*(1), 70-79.
11. Gao, G. P., Hu, B., Wang, S. F., & Yang, C. (2018). Wearable Circular Ring Slot Antenna With EBG Structure for Wireless Body Area Network. *IEEE Antennas and Wireless Propagation Letters*, *17*(3), 434-437.
12. Velan, S., Sundarsingh, E. F., Kanagasabai, M., Sarma, A. K., Raviteja, C., Sivasamy, R., & Pakkathillam, J. K. (2015). Dual-band EBG integrated monopole antenna deploying fractal geometry for wearable applications. *IEEE Antennas and Wireless Propagation Letters*, *14*, 249-252.
13. Gao, G., Hu, B., Wang, S., & Yang, C. (2018). Wearable planar inverted-F antenna with stable characteristic and low specific absorption rate. *Microwave and Optical Technology Letters*, *60*(4), 876-882.
14. Mersani, A., Osman, L., & Ribero, J. M. (2017). Performance of dual-band AMC antenna for wireless local area network applications. *IET Microwaves, Antennas & Propagation*, *12*(6), 872-878.
15. Lin, X., Seet, B. C., Joseph, F., & Li, E. (2018). Flexible Fractal Electromagnetic Bandgap for Millimeter-Wave Wearable Antennas. *IEEE Antennas and Wireless Propagation Letters*.
16. Peddakrishna, S., Khan, T., & De, A. (2017). Electromagnetic band-gap structured printed antennas: A feature-oriented survey. *International Journal of RF and Microwave Computer-Aided Engineering*, *27*(7), e21110.
17. H Rong, Q Wang, S Chen, Y Cao, H Tian. (2018). *Wide stopband miniaturized "I"-typed EBG with DGS*. *International Journal of RF and Microwave Computer Aided Engineering*.
18. Zhu, X. Q., Guo, Y. X., & Wu, W. (2016). A compact dual-band antenna for wireless body-area network applications. *IEEE Antennas Wireless Propag. Lett.*, *15*, 98-101.
19. Yan, S., Soh, P. J., & Vandenbosch, G. A. (2014). Low-profile dual-band textile antenna with artificial magnetic conductor plane. *IEEE Transactions on Antennas and Propagation*, *62*(12), 6487-6490.
20. Agarwal, K., Guo, Y. X., & Salam, B. (2016). Wearable AMC backed near-endfire antenna for on-body communications on latex substrate. *IEEE transactions on components, packaging and manufacturing technology*, *6*(3), 346-358.
21. Agneessens, S., Lemey, S., Vervust, T., & Rogier, H. (2015). Wearable, small, and robust: The circular quarter-mode textile antenna. *IEEE Antennas and Wireless Propagation Letters*, *14*, 1482-1485.
22. Raad, H. R., Abbosh, A. I., Al-Rizzo, H. M., & Rucker, D. G. (2013). Flexible and compact AMC based antenna for

telemedicine applications. *IEEE Transactions on antennas and propagation*, *61*(2), 524-531.

23. Jiang, Z. H., Cui, Z., Yue, T., Zhu, Y., & Werner, D. H. (2017). Compact, highly efficient, and fully flexible circularly polarized antenna enabled by silver nanowires for wireless body-area networks. *IEEE Trans. Biomed. Circuits Syst*, *11*(4), 920-932.
24. Velan, S., Sundarsingh, E. F., Kanagasabai, M., Sarma, A. K., Raviteja, C., Sivasamy, R., & Pakkathillam, J. K. (2015). Dual-band EBG integrated monopole antenna deploying fractal geometry for wearable applications. *IEEE Antennas and Wireless Propagation Letters*, *14*, 249-252.
25. Kim, S., Tentzeris, M. M., & Nikolaou, S. (2012, March). Wearable biomonitoring monopole antennas using inkjet printed electromagnetic band gap structures. In *Antennas and Propagation (EUCAP), 2012 6th European Conference on* (pp. 181-184). IEEE.
26. Salonen, P., & Rahmat-Samii, Y. (2006, November). Textile antennas: Effects of antenna bending on input matching and impedance bandwidth. In *Antennas and Propagation, 2006. EuCAP 2006. First European Conference on* (pp. 1-5). IEEE.
27. Yan, S., Soh, P. J., & Vandenbosch, G. A. (2014). Low-profile dual-band textile antenna with artificial magnetic conductor plane. *IEEE Transactions on Antennas and Propagation*, *62*(12), 6487-6490.
28. Pathak, P. P., Tripathi, H., & Kumar, V. (2010). Specific Absorption Rate Calculation and Rate of Temperature Change in Tissues Due to Radio Antenna. *International Transactions in Applied Sciences*, *2*(4).
29. Srinivasa Rao, Y., Ravikumar, G., Srinivasa Varma, P., "A new algorithm for the classification of faults in multi-terminal transmission network using wavelet morphology", International Journal of Recent Technology and Engineering, Vol. 7, No. 6, pp. 1102-1109, 2019.
30. *Patel PB, Shastri DH, Shelat PK, Shukla AK. "Ophthalmic Drug Delivery System: Challenges and Approaches." Systematic Reviews in Pharmacy 1.2 (2010), 114-120. Print. doi:10.4103/0975-8453.75042*
31. Veerabhadrappa, S., Baljoshi, V., Khanapure, S., Herur, A., Patil, S., Ankad, R., Chinagudi, S.Effect of yogic bellows on cardiovascular autonomic reactivity(2011) Journal of Cardiovascular Disease Research, 2 (4), pp. 223-227. DOI: 10.4103/0975-3583.89806